Crystalline Morphology and Thermal Properties for Random Copolyesters of (*R*)-3-Hydroxybutyric Acid with Different Hydroxyalkanoic Groups

*Hideki Abe and Yoshiharu Doi**

Polymer Chemistry Laboratory, RIKEN Institute, Hirosawa, Wako-shi, Saitama 351-0198, Japan

SUMMARY: The solid-state structures and thermal properties of melt-crystallized films of random copolymers of (*R*)-3-hydroxybutyric acid (3HB) with different hydroxyalkanoic acids such as (*R*)-3-hydroxypentanoic acid (3HV), (*R*)-3-hydroxyhexanoic acid (3HH), medium-chain-length (*R*)-3-hydroxyalkanoic acids (mcl-3HA; C8–C12), 4-hydroxybutyric acid (4HB), and 6-hydroxyhexanoic acid (6HH) were characterized by means of small-angle X-ray scattering, differential scanning calorimetry, and optical microscopy. The randomly distributed second monomer units except for 3HV in copolyesters act as defects of P(3HB) crystal and are excluded from the P(3HB) crystalline lamellae. The lamellar thickness of copolymers decreased with an increase in either the main-chain or the side-chain carbon numbers of second monomer units. In addition, the growth rate of spherulites decreased with an increase in the carbon numbers of second monomer units for copolymers with an identical comonomer composition. These results indicate that the steric bulkiness of second monomer unit affects on the crystallization of 3HB segments in random copolyesters.

Introduction

The poly[(*R*)-3-hydroxybutyric acid] (P(3HB)) and its copolymers, poly(hydroxyalkanoic acid)s (PHA), are produced from renewable carbon sources by a number of bacteria (Refs. 1–3). Since these PHA polymers are biodegradable thermoplastics, they have much attention as a new environmentally compatible material. A remarkable characteristic of PHA is their biodegradability in various environments. The biodegradation of PHA takes place on the surface of samples by the function of extracellular enzymes from microorganisms (Refs. 1, 2). To elucidate the mechanism of enzymatic hydrolysis of PHA materials with PHB depolymerases, the enzymatic reaction has been actively investigated using films (Refs. 4, 5) and single crystals (Ref. 6) of PHA. It has been demonstrated that the rate of biodegradation for PHA materials is strongly dependent both on the chemical structure of monomeric unit and on the solid-state structure of samples. In the aspect of the solid-state structure of PHA materials, the crystallinity and lamellar crystal sizes play a decisive role in degradation process (Ref. 7).

 CCC 1022-1360/00/$ 17.50+.50/0

In this study, we have attempted to obtain insight on the regulation of solid-state structure and thermal properties for various random copolymers with (*R*)-3-hydroxybutyric acid (3HB) unit as a constituent. The solid-state structures and thermal properties of melt-crystallized films for five types of random copolymers of 3HB with different hydroxyalkanoic acids are characterized by means of small-angle X-ray scattering, differential scanning calorimetry, and optical microscopy. The effect of second monomer structure on the solid-state structure and thermal properties are discussed.

Experimental Part

Poly[(*R*)-3-hydroxybutyric acid] (P(3HB)) homopolymer (Ref. 8) and five types of copolyesters; poly[(*R*)-3-hydroxybutyric acid-*co*-(*R*)-3-hydroxypentanoic acid] (P(3HB-*co*-3HV)) (Ref. 9), poly[(*R*)-3-hydroxybutyric acid-*co*-(*R*)-3-hydroxyhexanoic acid] (P(3HB-*co*-3HH)) (Ref. 9), poly[(*R*)-3-hydroxybutyric acid-*co*-medium-chain-length (*R*)-3-hydroxy-alkanoic acid] (P(3HB-*co*-mcl-3HA)) (Ref. 10), and poly[(*R*)-3-hydroxybutyric acid-*co*-4-hydroxybutyric acid] (P(3HB-*co*-4HB)) (Ref. 11), were prepared by the microbial synthetic methods. Poly[(*R*)-3-hydroxybutyric acid-*co*-6-hydroxyhexanoic acid] (P(3HB-*co*-6HH)) was synthesized by the ring-opening copolymerization of (*R*)-β-butyrolactone (e.e. 92 %) with ε-caprolactone (Ref. 12). By analysis of the ^{13}C nuclear magnetic resonance (NMR) spectra of copolyesters, the sequence distributions of 3HB and other hydroxyalkanoic acid units in all copolyesters were found to be statistically random. The melt-crystallized films of random copolyesters were prepared by isothermal crystallization at different temperatures of 30–140 °C for 3 days from the melt at 200 °C.

Differential scanning calorimetry (DSC) data of copolyester samples were recorded in the temperature range 0 to 200 °C on a PerkinElemer Pyris 1 equipped with a cooling accessory under a nitrogen flow of 20 ml·min^{-1}. Samples of 5 mg were encapsulated in aluminum pans and heated from 0 to 200 °C at a rate of 20 °C·min^{-1}. The melting temperature (T_m) and enthalpy of fusion (ΔH_m) were determined from the DSC endotherms. The T_m was taken as the peak temperature.

The small-angle X-ray scattering analyses of films were carried out at 27 °C using a Rigaku RINT 2500 system in the 2θ range 0.1–3.0 ° at a scan speed of 0.05 °·min^{-1}. Radiation of wavelength 0.154 nm (Cu Kα) was employed at a generator power of 40 kV and 200 mA.

The copolymer spherulitic morphologies were observed with a Nikon optical microscope equipped with crossed polarizers and a Linkham hot stage. The solvent-cast copolymer films (2 mg) were first heated on a hot stage from room temperature to 200 °C at a rate of 30 °C·min^{-1}. Samples were maintained at 200 °C for 30 s, and then the temperature was rapidly lowered to a given crystallization temperature (T_c) of 60–120 °C. The samples were crystallized isothermally at a given T_c to monitor the growth of the spherulites as function of

time. The radial growth rate of spherulites was calculated as the slope of the line obtained by plotting the spherulite radius against time with more than ten data points. For each crystallization measurement, the radial growth rate of the different three spherulites were recorded under the same conditions, and the spherulitic growth rates were averaged. During the thermal treatment, the copolymer films were kept under nitrogen flow in order to limit the degradation of the polymer. In order to minimize the risk of thermal degradation of copolymer, individual samples were used for each crystallization measurement.

Results and Discussion

Fig. 1 and Table 1 show the molecular structure, composition, glass-transition temperature, and molecular weight of copolymer samples used in this study. The melt-crystallized films of random copolyesters were prepared by isothermal crystallization at different temperatures of 30–140 °C for 3 days from the melt at 200 °C. After crystallization period of 3 days, all polyester films showed the well-developed and volume-filled spherulites. The melt-crystallized samples were subsequently allowed to stand at room temperature for 3 days before analytical measurements.

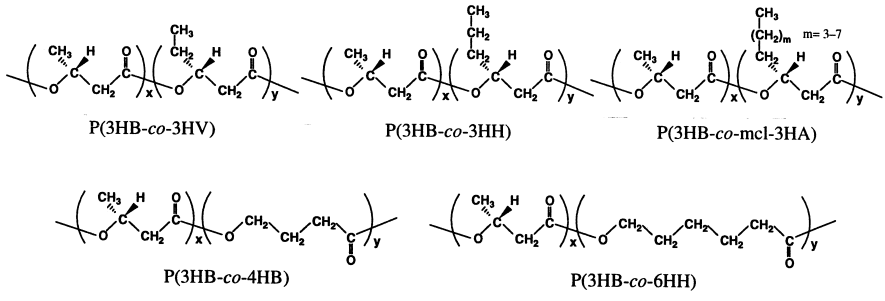

Fig. 1: Chemical structure of random copolymers of (*R*)-3-hydroxybutyric acid with different hydroxyalkanoic acids.

The thermal properties of melt-crystallized polyester films was characterized by differential scanning calorimetry (DSC). Two endothermic peaks were detected in the thermograms for several copolyester samples. In order to examine whether the peak at high temperature arises from a recrystallization process, the DSC curves of melt-crystallized films were recorded at different heating rates of 5–40 °C·min^{-1}. As the heating rate was increased, the higher temperature peak became smaller while the lower temperature peak area increased. The result indicates that the higher melting endothermic peak is caused by the rearrangement

Table 1. Molecular weights and glass-transition temperatures of polyester samples.

sample	molecular weight		glass-transition temperature
	$Mn \times 10^{-3}$	Mw/Mn	(Tg), °C
P(3HB)	300	2.3	4
P(3HB-*co*-6mol% 3HV)	183	2.4	0
P(3HB-*co*-6mol% 3HH)	350	2.7	-2
P(3HB-*co*-6mol% mcl-3HA)[a)]	605	2.3	-9
P(3HB-*co*-4mol% 4HB)	390	1.8	-1
P(3HB-*co*-8mol% 4HB)	197	1.9	-4
P(3HB-*co*-10mol% 4HH)	47	1.9	-5
P(3HB-*co*-10mol% 6HH)	107	1.7	-5

a) mcl-3HA units: 3-hydroxydecanoate (3 mol%), 3-hydroxydodecanoate (3 mol%), 3-hydroxyoctanoate (< 1 mol%), 3-hydroxy-cis-5-dodecenoate (< 1 mol%)

of an initial crystal morphology of copolyester. The lower melting temperature represents the melting of original crystals formed at a crystallization temperature.

Fig. 2 shows the melting temperature of random copolymers crystallized at various temperatures. For all copolymer samples, the melting temperature rose with crystallization temperature, suggesting that the thickness of crystalline lamellae in melt-crystallized polyester films increases with an increase in the crystallization temperature. The melting temperature of copolymers depressed as the second monomer fraction was increased. It is of interest to note that the melting temperatures of melt-crystallized films for random copolymers vary with chemical structure of second monomer units, when the values are compared among the copolymers with an identical second monomer composition crystallized at same temperature. The melting temperatures of P(3HB-*co*-6mol% 3HH) films were higher than those of P(3HB-*co*-6mol% mcl-3HA) films, while those were lower than the values of P(3HB-*co*-6mol% 3HV) films, indicating that the melting temperature decreases with side-chain length of second monomer unit (as shown in Fig. 2 (a)). The melting tempertatures of P(3HB-*co*-10mol% 4HB) films were higher than those of P(3HB-*co*-10mol% 6HH) films, indicating that the melting temperature decreases with main-chain length of second monomer unit (as shown in Fig. 2 (b)).

The lamellar structure of melt-crystallized polyester films were characterized by the small-angle X-ray scattering (SAXS) technique. The lamellar thickness (l_c) of the melt-crystallized samples were calculated from the SAXS data according to the pseudo two-phase model using one-dimensional correlation function which can be taken directly as the Fourier transform of the scattering intensity (Refs. 13, 14). The l_c value of P(3HB) samples increased from 5.3 nm to 8.2 nm with an increase in crystallization temperature. The l_c values of P(3HB-*co*-6mol% 3HV) ranged in 4.1–8.5 nm, and the values were almost consistent with the value of P(3HB) homopolymer at a given crystallization temperature. For the other copolyester samples, the l_c values ranged in 1.6–4.5 nm, and the values tended to increase with

crystallization temperature. In addition, the l_c values for copolyesters except for P(3HB-*co*-3HV) thinned down with an increase in second monomer fraction.

The reduction in melting temperature from an equilibrium value is accounted for in terms of the limited lamellar thickness and may be expressed theoretically by the Gibbs-Thomson equation (1):

$$T_m = T_m^0 \left(1 - \frac{2\sigma_e}{\Delta H_m \cdot l_c} \right) \qquad (1)$$

where T_m is the observed melting temperature, T_m^0 is the equilibrium melting temperature, σ_e is the fold surface free energy, ΔH_m is the heat of fusion, and l_c is the lamellar thickness. Fig. 3 shows the relationship between the inverse lamellar thickness ($1/l_c$) and the melting temperature (T_m) of melt-crystallized polyester samples; P(3HB), P(3HB-*co*-6mol% 3HV), P(3HB-*co*-6mol% 3HH), P(3HB-*co*-6mol% mcl-3HA), P(3HB-*co*-4mol% 4HB) and P(3HB-*co*-10mol% 4HB). The plot of melting temperature against inverse lamellar thickness for P(3HB) homopolymer shows the linear relationship. From the intercept of the line, we can find that the equilibrium melting temperature of P(3HB) is 194 °C. For P(3HB-*co*-6mol% 3HV) sample, the line shifted lower melting temperatures at the same lamellar thickness compared to P(3HB) homopolymer, and the equilibrium melting temperature was 185 °C. On the other hand, the plots of T_m against $1/l_c$ for the other copolymers fitted with the line obtained from plotting the T_m and $1/l_c$ of P(3HB) samples extrapolating toward thinner lamellar thickness.

It has been well-known that the P(3HB-*co*-3HV) copolymers show the isodimorphism due to the cocrystallization of 3HB and 3HV units in the composition range from 0 to 30 mol% of 3HV units (Ref. 15). The observed shift to lower temperature of the relation curve between melting temperature against inverse lamellar thickness for P(3HB-*co*-3HV) with respect to P(3HB) is attributed to the incorporation of 3HV units in P(3HB) crystalline lattice (Ref. 7). In contrast, the other second monomer units are completely excluded from the P(3HB) crystalline lattice. The crystalline structure of lamellae for 3HB-based copolyesters except for P(3HB-*co*-3HV) is essentially the same as that for P(3HB) homopolymer, and the depression of melting temperature is attributed to the decrease in lamellar thickness. The melting temperatures of melt-crystallized films decreased with carbon numbers of second monomer units for copolymers with an identical second monomer composition crystallized at same temperature (as shown in Fig. 2). Consequently, the lamellar thickness of copolymers decreased with an increase in either the main-chain or the side-chain carbon numbers of second monomer unit.

The crystallization kinetics of random copolymers were studied without adding nucleating agents. The spherulites of copolymers were observed with a polarized optical microscope as a function of time at a given temperature. The samples were isothermally crystallized at a temperature between 50 and 120 °C after melting at 200 °C for 30 s. The spherulite radius increased linearly with time. The radial growth rate of spherulites was calculated as the slope of the line obtained by plotting the spherulite radius against time. Fig. 4

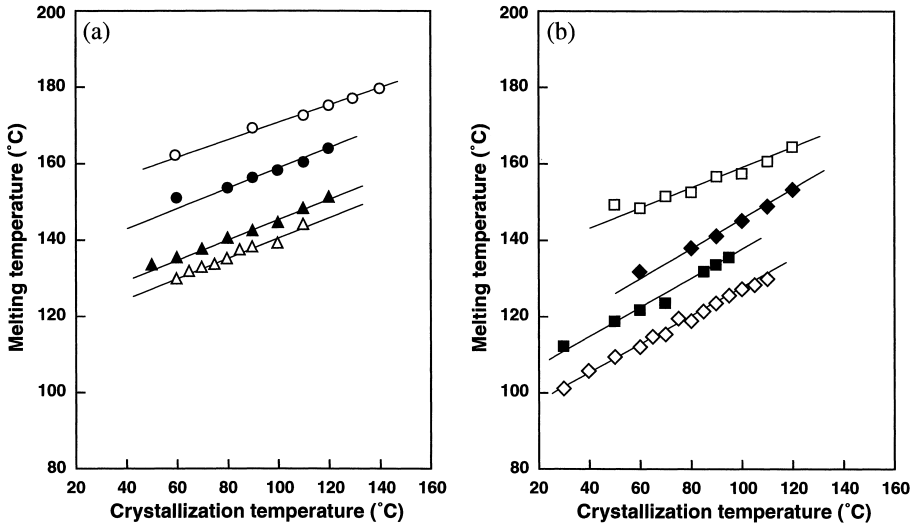

Fig. 2: Melting temperature (T_m) of melt-crystallized copolyester films crystallized at various temperatures. (a) (○): P(3HB), (●): P(3HB-*co*-6mol% 3HV), (▲): P(3HB-*co*-6mol% 3HH), and (△): P(3HB-*co*-6mol% mcl-3HA), (b) (□): P(3HB-*co*-4mol% 4HB), (◆): P(3HB-*co*-8mol% 4HB), (■): P(3HB-*co*-10mol% 4HB), and (◇): P(3HB-*co*-10mol% 6HH).

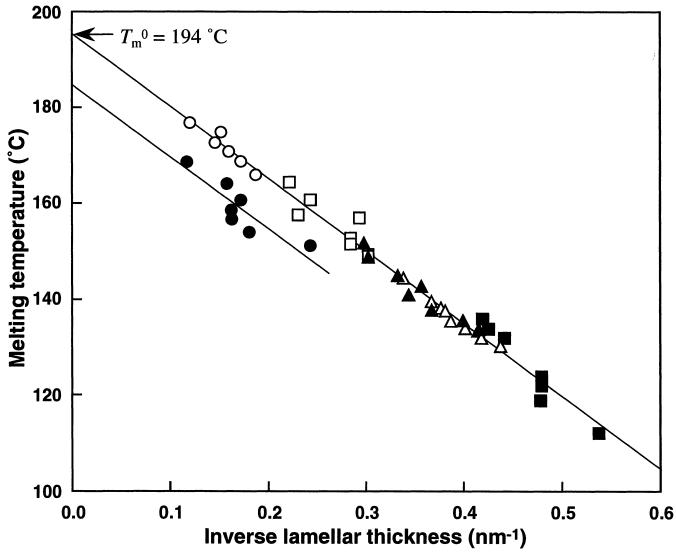

Fig. 3: Variation in melting temperature (T_m) as a function of the inverse lamellar thickness ($1/l_c$) for melt-crystallized polyester films. (○): P(3HB), (●): P(3HB-*co*-6mol% 3HV), (▲): P(3HB-*co*-6mol% 3HH), (△): P(3HB-*co*-6mol% mcl-3HA), (□): P(3HB-*co*-4mol% 4HB), and (■): P(3HB-*co*-10mol% 4HB).

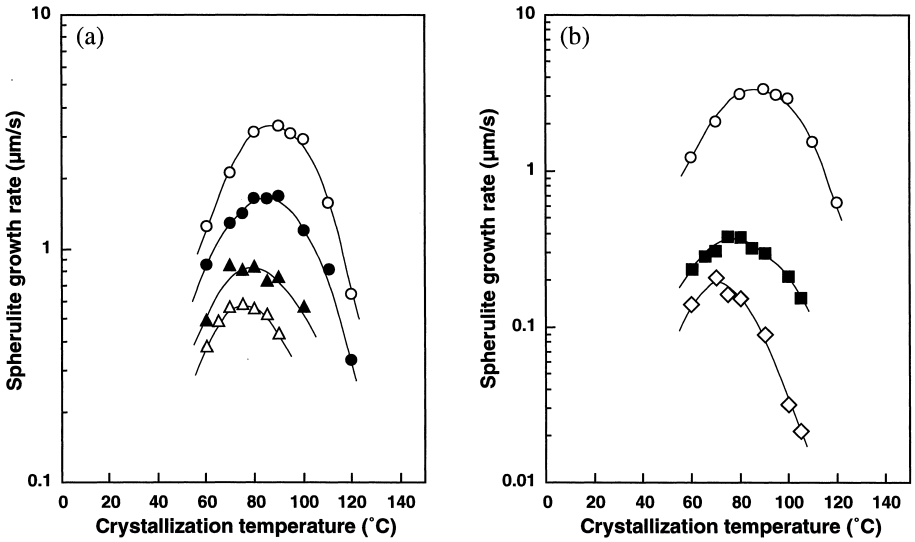

Fig. 4: Radial growth rate (G) of spherulites as a function of crystallization temperature (T_c). (a) (○): P(3HB), (●): P(3HB-*co*-6mol% 3HV), (▲): P(3HB-*co*-6mol% 3HH), and (△): P(3HB-*co*-6mol% mcl-3HA), (b) (○): P(3HB), (■): P(3HB-*co*-10mol% 4HB) and (◇): P(3HB-*co*-10mol% 6HH).

(a) shows the radial growth rate of spherulites at different crystallization temperatures for various polyester samples; P(3HB), P(3HB-*co*-6mol% 3HV), P(3HB-*co*-6mol% 3HH), and P(3HB-*co*-6mol% mcl-3HA). A maximum value of 3.4 μm/s was observed around 90 °C for P(3HB) homopolymer. The spherulitic growth rates were reduced by the incorporation of second monomer units into 3HB sequences even for P(3HB-*co*-3HV) copolymer. As it can be seen from Fig. 4 (a), the spherulitic growth rates for copolymers containing 6 mol% second monomer units were reduced as the side-chain length of second monomer increased. In addition, the crystallization curves of copolymers were shifted toward lower temperatures.

Fig. 4 (b) shows the radial growth rates for P(3HB-*co*-10mol% 4HB) and P(3HB-*co*-10mol% 6HH) copolymers. The growth rate of spherulites reduced with an increase of the carbon number of main-chain length of second monomer units. It is noted from the result of Fig. 4 that the growth rate of spherulites decreased with an increase in the side-chain length or main-chain length of second monomer units for copolymers with an identical monomer composition. These results indicate that the sterically bulky structure of second monomer units in copolyesters efficiently hinders the crystallization of 3HB segments. The randomly distributed second monomer units in copolymers may be responsible for the remarkable decrease in the transport rate of 3HB segments at the growth front of crystalline lamellae.

It has been concluded that the randomly distributed second monomer units except for 3HV in 3HB-base copolyesters act as defects of P(3HB) crystal and are completely excluded from the P(3HB) crystalline lamellae. During the crystallization process, second monomer units prevent the crystallization of 3HB segments in random copolyesters. The steric bulkiness of second monomer unit is responsible for hindrance of crystallization for 3HB segments in random copolyesters.

(1) P.A. Holmes, "*Developments in Crystalline Polymers—2*", (Ed. Bassett, D. C.), Elsevier, London 1988

(2) Y. Doi Y, "Microbial Polyesters", VCH Publishers: New York 1990

(3) A.J. Anderson, E.A. Dawes, *Microbiol. Rev.* **54**, 450 (1990)

(4) H. Abe, Y. Doi, *Int. J. Biol. Macromol.* **25**, 185 (1999)

(5) H. Abe, Y. Kikkawa, T. Iwata, H. Aoki, T. Akehata, Y. Doi, *Polymer* **41**, 867 (2000)

(6) T. Iwata, Y. Doi, *Macromol. Chem. Phys.* **200**, 2429 (1999)

(7) H. Abe, Y. Doi, H. Aoki, T. Akehata, *Macromolecles* **31**, 1791 (1998)

(8) Y. Doi, A. Tamaki, M. Kunioka, K. Soga, *Appl. Microbiol. Biotechnol.* **28**, 330 (1988)

(9) Y. Doi, S. Kitamura, H. Abe, *Macromolecules* **28**, 4822 (1995)

(10) H. Matsusaki, H. Abe, Y. Doi, *Biomacromolecules* **1**, 17 (2000)

(11) S. Nakamura, Y. Doi, M. Scandola, *Macromolecules* **25**, 4237 (1992)

(12) H. Abe, Y. Doi, H. Aoki, T. Akehata, Y. Hori, A. Yamaguchi, *Macromolecules* **28**, 7630 (1995)

(13) C.G. Vonk, *J. Appl. Crystallogr.* **8**, 340 (1975)

(14) R. Verma, H. Marand, B. Hsiao, *Macromolecules* **29**, 7767 (1996)

(15) S. Bloembergen, D.A. Holden, G.K. Hamer, T.L. Bluhm, R.H. Marchessault, *Macromolucules* **19**, 2865 (1986)